Journal of Fundamental and Applied Sciences

Research Article

ISSN 1112-9867

Available online at http://www.jfas.info

IMPACT OF SIMULATION MODEL AND GRAIN SIZE ON THE BIFACIAL GAIN OF A SILICON SOLAR CELL

Esso-Ehanam Tchedre[1], Boubacar Soro[1,2*], Guy Serge Tchouadep[1], Mahamadi Savadogo[1], Issa Zerbo[1] and Martial Zoungrana[1]

[1]Laboratory of Thermal and Renewable Energies, Universite Joseph KI-ZERBO, Ouagadougou, Burkina Faso

[2]Institut des Sciences et Technologie, Ecole Normale Supérieure, Ouagadougou, Burkina Faso

Received: 15 August 2024 / Accepted: 21 Decembre 2024 / Published: 22 Decembre 2024

ABSTRACT

The characterisation of the performance of a bifacial silicon cell in a simulation study is carried out through different simulation models. These are the one-dimensional (1D) model, the classical three-dimensional model using constant diffusion parameters and the empirical 3D model which uses diffusion parameters varying with grain size. For each of these models, by comparing the electrical parameters of the solar cell subjected to front side illumination and then to double illumination, the different bifacial gains are obtained and then compared to each other. This study revealed a tendency for the classical 1D and 3D models to overestimate the bifacial gains compared to the empirical 3D model.

Keywords: Silicon bifacial solar cell; study models; grain size; electrics parameters.

Author Correspondence, e-mail: soro.bo@gmail.com

doi: http://dx.doi.org/10.4314/jfas.1381

1. INTRODUCTION

Bifacial solar cells are designed to receive solar radiation from both sides. Bifacial cells are thus one of the solutions in the quest for better exploitation of the huge solar resource. Today, bifacial technology is increasingly being adopted. Thus, the market share of bifacial panels is constantly approaching that of their conventional single-sided cell equivalent [1]. Nevertheless, research in the field of bifacial solar needs to continue in order to improve their efficiency and thus make them more competitive.

In the quest to improve the performance of bifacial cells, it is imperative to develop appropriate simulation tools. It is in this context that this study aims to conduct a comparative study on the electrical parameters of a bifacial silicon solar cell under different simulation models. As the cell is subjected to constant multispectral illumination, the study aims to compare the different bifacial gains obtained when switching from front side illumination to simultaneous illumination of both sides. This study is carried out using the classical 1D and 3D simulation models [2,3,4] which make use of constant charge carrier diffusion parameters and the so-called empirical 3D model [5,6] because it makes use of a diffusion length and a charge carrier lifetime that increases with the grain size of the material. The electrical parameters studied are the short-circuit photocurrent (Jsc), open-circuit photovoltage (Vco), the (P-V) characteristic, fill factor (F.F) and the conversion efficiency.

The aim of this study is to choose, among those three simulation models, the one most suitable for the simulation of the performance strongly linked to the bifacial character of the solar cell.

2. ANALYTICAL FORMULATION AND DETERMINATION OF ELECTRICAL PARAMETERS

The solar cell studied is a bifacial n-p-p+ polycrystalline silicon cell subjected to constant polychromatic illumination in the AM 1.5 condition. The representation of the solar cell in a one-dimensional (1-D) model is given in figure 1. In this model, the cell is considered as a single grain with the thickness of the cell neglected compared to its lateral dimensions. In the three-dimensional (3-D) model, in the approximation of the columnar model, the solar cell is assumed to be made up of a parallel juxtaposition of identical grains separated by boundaries.

This model then leads to take into account the size of the columnar grains and the possibility of charged carriers losses at the grain boundaries (g) characterised by the grain boundary recombination rate (Sgb). The three-dimensional (3-D) representation of the solar cell is shown in Figure 2.

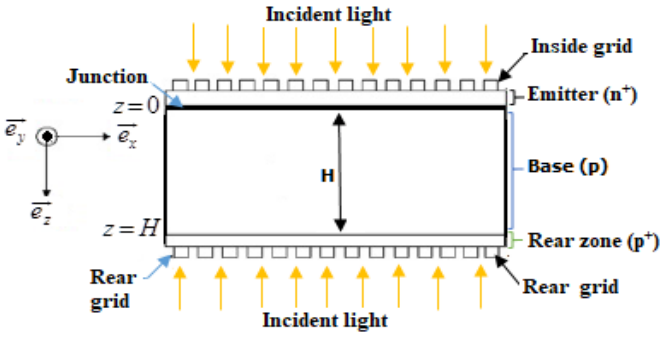

Fig.1. One-dimensional model of silicon solar cell under double illumination

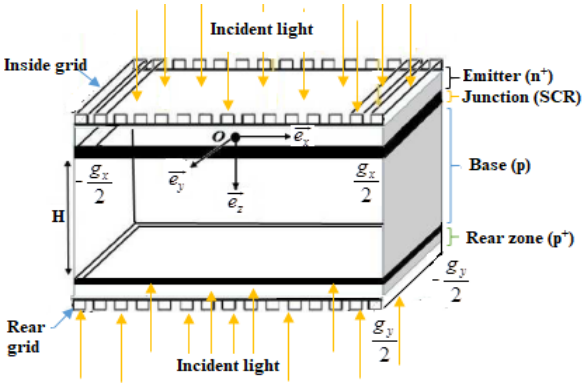

Fig.2. Three-dimensional model of an isolate silicon solar cell under double illumination

Whatever the study model, we make the following assumptions:

- The contribution of the emitter is neglected; the study is thus reduced to that of the base of the cell and the origin of the axis system is taken at the junction
- The base is assumed to be a quasi-neutral region [7].
- The generation rate depends only on the depth z of the base.

In the particular case of 3D models, the following assumptions are added to these:

- In the approximation of the 3D columnar model considered, the grain boundaries are recombination planes perpendicular to the junction [7, 8].
- The diffusion parameters (D_n and L_n) remain constant and independent of the grain size in the classical 3D model.
- In the empirical 3D model, only the diffusion coefficient (D_n) and the mobility (μ_n) are constant [5, 6]. The diffusion length of the carriers (L_n) is related to the grain size (g) by equation (1) [6]:

$$\frac{1}{L_n(g)^2} = 1.11\times10^3 + 4\times\frac{10^2}{g} \quad (1)$$

In the static regime, according to the model, the density of excess minority charge carriers obeys to the following equations:

- **One-dimensional model (1D),**

$$\frac{\partial^2\delta(z)}{\partial z^2} - \frac{\delta(z)}{L_n{}^2} = -\frac{G(z)}{D_n} \quad (2)$$

- **Three-dimensional model (3D),**

$$\frac{\partial^2\delta(x,y,z)}{\partial^2 x} + \frac{\partial^2\delta(x,y,z)}{\partial y^2} + \frac{\partial^2\delta(x,y,z)}{\partial z^2} - \frac{\delta(z)}{L_n{}^2} = -\frac{G(z)}{D_n} \quad (3)$$

In these equations (2) et (3), τ_n, L_n and D_n represent respectively the lifetime, the diffusion length and the diffusion coefficient of electrons. These are linked by the following relationship:

$$L_n{}^2 = \tau_n . D_n \quad (4)$$

For both 1D and 3D models, the generation rate depends only on the depth z of the base:

- Front illumination $G_1(z) = \sum_{i=1}^{3} a_i e^{-b_i(z)}$ (5)

- Double illumination $G_2(z) = \sum_{i=1}^{3} a_i e^{-b_i(H-z)}$ (6)

a_i and b_i are coefficients deduced from modeling of the generation rate considered for overall the solar radiation spectrum when AM=1.5 [9, 10].

Solving the continuity equations gives the charge carrier density expressions. According to the study model, from these charge carrier density expressions, the photocurrent density is deduced by the equations (7) and (8) [11]:

- **one- dimension model (1-D)**:

$$J_{ph} = qD_n \left.\frac{\partial\delta(z)}{\partial z}\right|_{z=0} \quad (7)$$

- **three-dimension model (3-D):**

$$J_{ph}^{*} = \frac{q \cdot D_n}{g_x \cdot g_y} \int_{-g_x/2}^{g_{x/2}} \int_{-g_y/2}^{g_y/2} \left[\frac{\partial \delta^{*}(x,y,z,g)}{\partial z} \right]_{z=0} dx \cdot dz \qquad (8)$$

The photovoltage are deduced respectively by the equations (9) and (10) [2, 13]:

- **One- dimension model (1-D):**

$$V_{ph} = V_T \cdot \ln\left[1 + \frac{N_B \times \delta(0)}{n_i^2}\right] \qquad (9)$$

- **Three-dimension model (3-D):**

$$V_{ph}^{*} = V_T \ln\left[1 + \frac{N_B}{n_i^2} \int_{-g_x/2}^{g_x/2} \int_{-g_y/2}^{g_y/2} \delta^{*}(x,y,0,g)\, dxdy\right] \qquad (10)$$

Where q is electric charge, V_T is the thermal voltage given by: $V_T = \frac{k_B.T}{q}$, n_i represents the intrinsic carrier concentration, with $n_i = 10^{10}\, cm^{-3}$ for silicon, N_B is the base doping density ($N_B = 10^{16} cm^{-3}$) and k_B is the Boltzmann's constant.

From the expressions for photocurrent and photovoltage, for both 1D and 3D models, the electrical power (P_{el}), fill factor (FF) and conversion efficiency (η) are determined by equations (11), (12) and (13) respectively [14]:

$$P_{el} = J_{ph} \cdot V_{ph} \qquad (11)$$

$$FF = \frac{J_{\max}.V_{\max}}{J_{SC}.V_{OC}} = \frac{P_{\max}}{J_{SC}.V_{OC}} \qquad (12)$$

$$\eta = \frac{P_{\max}}{P_{inc}} = \frac{FF \cdot J_{SC} \cdot V_{OC}}{P_{inc}} \qquad (13)$$

$J_{\max}$ and $V_{\max}$ are respectively the photocurrent and photovoltage at the point of maximum power; $P_{\max}$ are maximum power with $P_{\max} = J_{\max} \times V_{\max}$. J_{SC} and V_{OC} are respectively the short-circuit photocurrent and open-circuit photovoltage. P_{inc} is the power of the incident light, referred to standard conditions of Mass Air 1.5 and temperature equal to 25°C. Its

normalised value is $P_{inc} = 100\ mW/cm^2$.

3. RESULTS AND DISCUSSIONS

Figures 2-a and 2-b compare the J-V characteristics of illumination from the front and double illumination resulting from the 3D model and for different grain sizes of the classical and empirical 3D models.

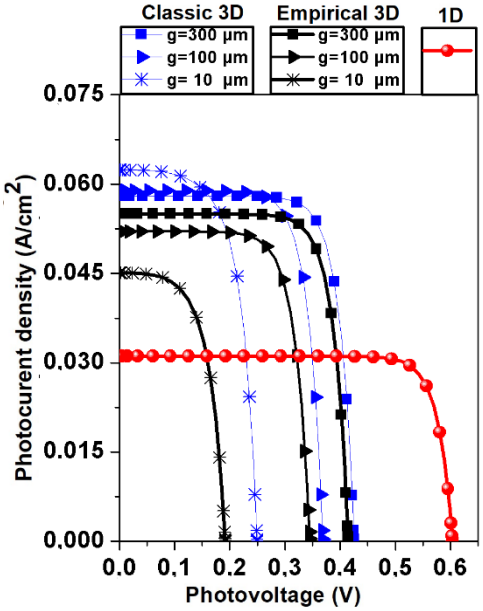

Fig.2a. J-V characteristic in 1D, classic 3D and empirical 3D models at front illumination:

$S_b = 10^3 cm/s, L_n = 0.015cm, H = 0.03cm.$

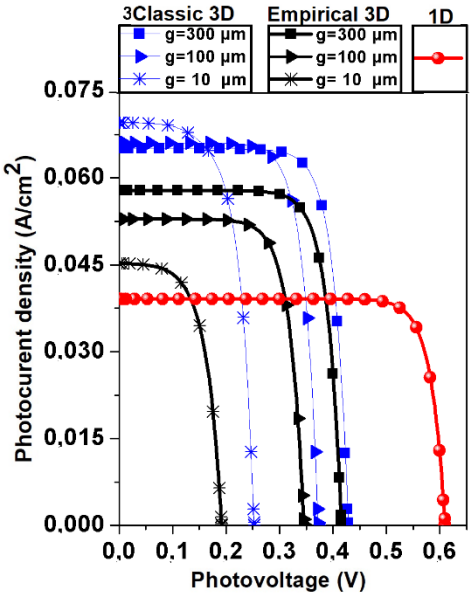

Fig.2b. J-V characteristic in 1D, classic 3D and empirical 3D models at double illumination:

$S_b = 10^3 cm/s, L_n = 0.015cm, H = 0.03cm.$

For all three simulation models, Figures 2-a and 2-b show an increase in the short-circuit photocurrent from front illumination to double illumination. This increase in short-circuit photocurrent at double illumination is clearly noticeable in the 1D model. This increase in short-circuit photocurrent is also quite noticeable in the classical 3D model. In the empirical 3D model, the gain in photocurrent is only noticeable with increasing of the grain size.

Furthermore, in contrast to the classic 3D model, in the empirical 3D model, the increase in grain size leads to an increase in the short-circuit photocurrent. This result is in the logic of a reduction of the charge carrier losses with the increase of the grain size which leads to a

reduction of the grain boundaries.

The same figures show that the open circuit photovoltage remains very little affected by the switch to double illumination.

Figures 3-a and 3-b compare the P-V characteristics of illumination from the front and double illumination resulting from the 3D model and for different grain sizes of the classical and empirical 3D models.

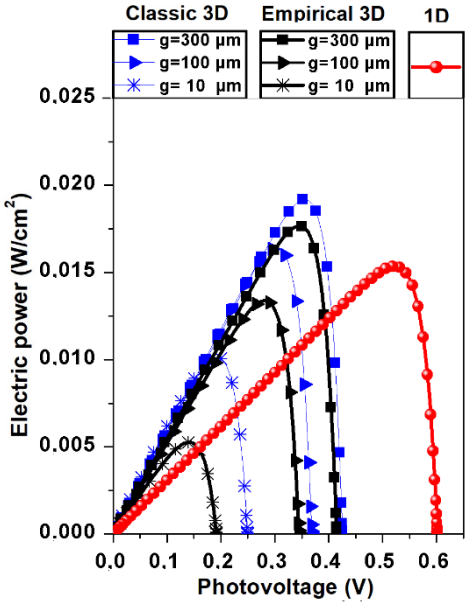

Fig.3a. P-V characteristic in 1D, classic 3D and empirical 3D models at front illumination:

$S_b = 10^3 cm/s, L_n = 0.015cm, H = 0.03cm.$

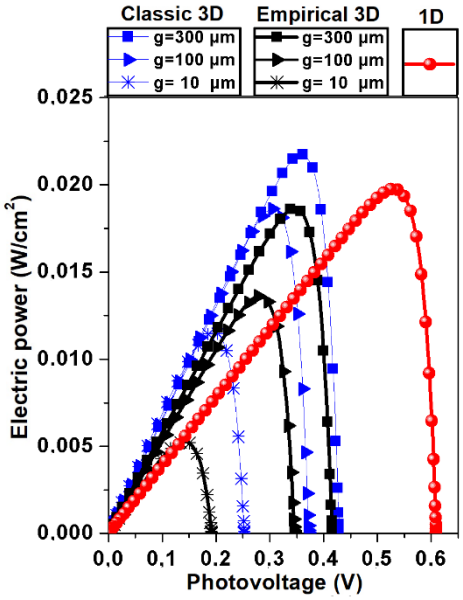

Fig.3b. P-V characteristic in 1D, classic 3D and empirical 3D models at double illumination:

$S_b = 10^3 cm/s, L_n = 0.015cm, H = 0.03\,cm.$

These figures show that for the same photovoltage, from front illumination to double illumination, there is an increase in electric power. In particular, for the maximum power, its increase at double illumination is quite clearly noticeable in the 1D and 3D empirical models. This increase in maximum power at double illumination is less significant in the 3D empirical model and is more noticeable with increasing of the grain size.

Figures 4-a and 4-b compare conversion efficiencies of illumination from the front and double illumination resulting from the 1D model and those obtained as a function of grain size in the two 3D models.

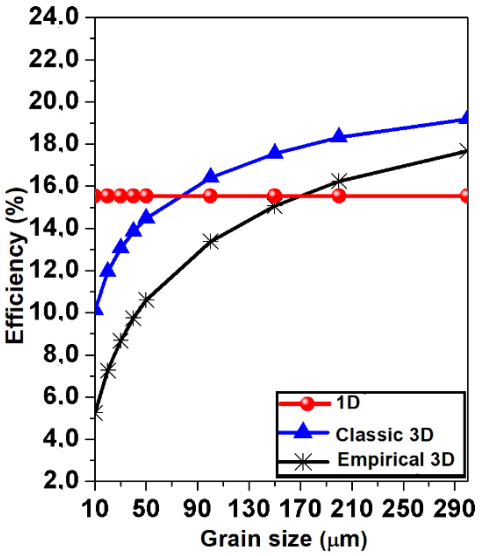

Fig.4a. Conversion efficiency in 1D, classic 3D and empirical 3D models at front illumination:

$S_b = 10^3 cm/s, L_n = 0.015cm, H = 0.03cm.$

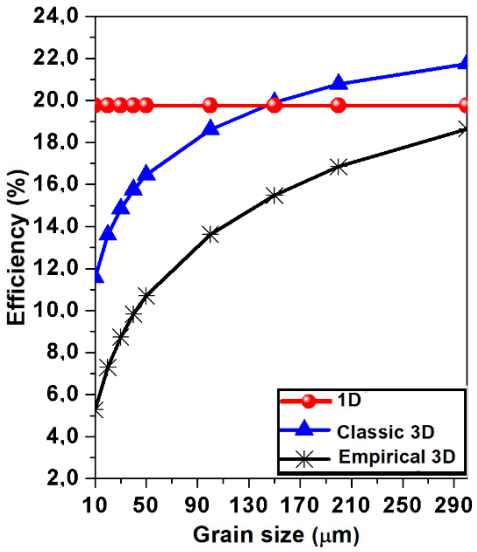

Fig.4b. Conversion efficiency in 1D, classic 3D and empirical 3D models at double illumination:

$S_b = 10^3 cm/s, L_n = 0.015cm, H = 0.03cm.$

These figures show that when switching from front illumination to double illumination, there is an increase of efficiency for all simulation models. This result is in agreement with the increase in maximum power obtained earlier. As observed in the case of power, the bifacial gain in efficiency is very noticeable in the 1D model. For the same grain size, the efficiency gain is more noticeable in the classic 3D model compared to the empirical 3D model.

Furthermore, it is observed that for both 3D models, the increase in grain size leads to an increase in efficiency. Moreover, the classic 3D model overestimates the conversion efficiency compared to the empirical 3D model. Finally, at front illumination, compared to the two 3D models, the 1D model overestimates the performance for grain sizes below about 80 µm in the classic 3D model and at about 180 µm. However, at double illumination, for the grain size limits considered in this study, the efficiency resulting from the 1D model is overestimated compared to the 3D empirical model. Compared to the classic 3D model, resulting from of the 1D model is only overestimated for grain sizes below about 150 µm.

Figures 5-a and 5-b compare form factors of illumination from the front and double illumination resulting from the 1D model and those obtained as a function of grain size in the two 3D models.

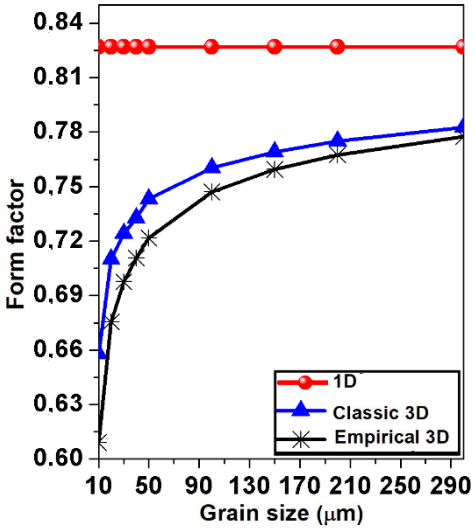

Fig.5a. Form factor in 1D, classical 3D and empirical 3D models at front illumination:

$S_b = 10^3 cm/s, L_n = 0.015cm, H = 0.03cm.$

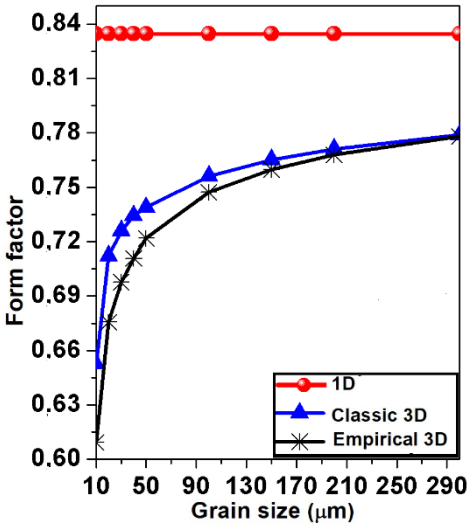

Fig.5b. Form factor in 1D, classical 3D and empirical 3D models at double illumination:

$S_b = 10^3 cm/s, L_n = 0.015cm, H = 0.03cm.$

Comparison of these two figures shows a small increase in the fill factor resulting from the 1D model when switching to double illumination. From the same figures, it appears that the effect of switching to double illumination is hardly noticeable across the two 3D models.

Furthermore, it is observed that, as for the efficiency, for all 3D models, the increase in grain size leads to a significant increase in the efficiency independently of the illumination mode. Moreover, the classic 3D model overestimates the fill factor compared to the empirical 3D model. This fill factor is greatly overestimated by the 1D model compared to the two 3D models.

For the different electrical parameters studied, the following table gives the different bifacial gains resulting from the 1D model and those obtained for different grain sizes in the two 3D models.

Over the grain size range considered in this study, this table shows that compared to the empirical 3D model, the 1D and classic 3D models tend to overestimate the bifacial gain obtained on short circuit photocurrent, maximum power and efficiency. Compared to the classic 3D model, the 1D model in turn tends to overestimate the bifacial gain obtained on the same electrical parameters.

Table 1. Different bifacial gains resulting from the 1D model and those obtained for different grain sizes in the two 3D models

Model	Grain size (μm)	J_{SC} gain $\frac{J_{SC2}-J_{SC1}}{J_{SC2}}$ (%)	V_{OC} gain $\frac{V_{OC2}-V_{OC1}}{V_{OC2}}$ (%)	P_{max} gain $\frac{P_{max2}-P_{max1}}{P_{max2}}$ (%)	η gain $\frac{\eta_2-\eta_1}{\eta_2}$ (%)	FF gain $\frac{FF_2-FF_1}{FF_2}$ (%)
1D		26.71	1.31	27.15	27.15	0.15
Classic	*10*	11.58	1.30	14.05	14.05	0.89
3D	*100*	12.26	0.89	13.46	13.46	0.18
	300	12.26	0.77	13.28	13.28	0.14
Empirical	*10*	0.29	0.04	0.34	0.34	0.02
3D	*100*	1.61	0.12	2.74	2.74	0.03
	300	5.19	0.26	5.54	5.54	0.05

For these three simulation models, the bifacial gain on the open circuit photovoltage can be considered negligible compared to that obtained on the photocurrent, which in turn affects the electrical power and efficiency.

Concerning the fill factor, the bifacial gains, although small, have a significant impact on the performance of the solar cell and cannot be neglected. So, over the range of grain sizes considered, the classic 3D model gives the highest gain on the fill factor, followed by the 1D model.

Finally, the same table shows that the increase in grain size leads to an increase in the bifacial gain resulting from the empirical 3D model. This result, which is more logical, is explained by the reduction of charge carrier losses at the grain boundaries as the grain size increases. In contrast, in the classic 3D model, this same increase in grain size has little impact on the bifacial gain, which in fact shows a slight downward trend. This notable difference obtained on the impact of the grain size on the bifacial gain is caused by the taking into account by the empirical 3D model of the effect of the grain size on the diffusion length of the charge carriers contrary to the classic 3D model.

4. CONCLUSION

A comparative study was made to investigate the impact of the simulation model and the grain size on the bifacial gain of a polycrystalline silicon solar cell. This study is done in the static regime under constant multispectral illumination. The models used are the classic 1D and 3D models using constant diffusion parameters and empirical 3D model which uses a diffusion length increasing with grain size.

The study shows that for all three simulation models, when switching from front illumination to double illumination, there is a significant increase in short-circuit photocurrent, maximum power and conversion efficiency. Compared to the two 3D models, the 1D model overestimates the bifacial gains obtained on these different parameters. The classic 3D model in the same way, overestimates the bifacial gains in comparison with the empirical 3D model.

For the three models studied, the bifacial gain on the open circuit photovoltage and the fill factor remain very low. For the fill factor in particular, the gain, although very small, is not to be neglected regard of its impact on the performance of the solar cell. The classic 3D model thus leads to the highest bifacial gain on fill factor (0.9%), followed by the 1D model (0.15%) and the empirical 3D model (0.05%). The bifacial gain obtained on the maximum power and conversion efficiency can be considered as essentially due to the photocurrent because the gain on the photovoltage in particular of open circuit remains very low.

In view of all the results obtained in this work, although the empirical 3D model leads to lower bifacial gains compared to the other two models, its use would be more appropriate in the prediction of the performance of a bifacial solar cell.

5. ACKNOWLEDGEMENTS

The authors wish to thank International Science Program (ISP) for funding our research group and allowing to conduct these works.

6. REFERENCES

[1] R. Kopecek and J. Libal. Bifacial photovoltaics 2021: Status, opportunities and challenges.

Energies, **2021**, 14(8):2076.

[2] G.S. Tchouadep, E.K. Tchédré, I. Sourabié, I. Zerbo, and M. Zoungrana. Modelling the influence of low energy electrons emitted from pm-147 on the performance of a silicon pv cell. International Journal of Innovation and Applied Studies, **2022**, 36(1):205–212.

[3] M. Dieye, S. Mbodji, M. Zoungrana, I. Zerbo, B. Dieng, and G. Sissoko. A 3D Modelling of Solar Cell's Electric Power under Real Operating Point. World Journal of Condensed Matter Physics, **2015**, 05(04):275–283.

[4] G. Sahin. Effect of temperature on the series and shunt resistance of a silicon solar cell under frequency modulation. Journal of Basic and Applied Physics, **2016**, 5(1):21–29.

[5] A. K. Ghosh, C. Fishman, and T. Feng. Theory of the electrical and photovoltaic properties of polycrystalline silicon. Journal of Applied Physics, **1980**, 51(1):446–454.

[6] M. Imaizumi, T. Ito, M. Yamaguchi, and K. Kaneko. Effect of grain size and dislocation density on the performance of thin film polycrystalline silicon solar cells. Journal of applied physics, **1997**, 81(11):7635–7640.

[7] N. C. Halder and T. R. Williams. Grain boundary effects in polycrystalline silicon solar cells. Solution of the three-dimensional diffusion equation by the green's function method. Solar Cells, **1983**, 8(3):201–223.

[8] J. Dugas and J. Oualid. 3D-modelling of polycrystalline silicon solar cells. Revue de Physique Appliquée, **1987**, 22(7):677–685.

[9] M. Chen and C.-Y. Wu. A new method for computer-aided optimization of solar cell structures. Solid-state electronics, **1985**, 28(8):751–761.

[10] J. Furlan and S. Amon. Approximation of the carrier generation rate in illuminated silicon. Solid-state electronics, **1985**, 28(12):1241–1243.

[11] F. I. Barro and M. Sané. Effect of both magnetic field and doping density on series and shunt resistances under frequency modulation. Indian Journal of Pure and Applied Physics, **2015**, 53:590–595.

[12] J. Dugas and J. Oualid. A model of the dependence of photovoltaic properties on effective diffusion length in polycrystalline silicon. Solar Cells, **1987**, 20(3):167–176.

[13] M. Zoungrana, I. Zerbo, F. Ouedraogo, B. Zouma, and F. Zougmoré. 3d modelling of

magnetic field and light concentration effects on a bifacial silicon solar cell illuminated by its rear side, **2012**, 29(1):12–20.

[14] E. Lorenzo. Solar electricity: engineering of photovoltaic systems. Earthscan/James James, **1994.**